Journal of The Electrochemical Society, **159** (3) H290-H292 (2012)
0013-4651/2012/159(3)/H290/3/$28.00 © The Electrochemical Society

Growth and Characteristics of *a*-Plane GaN on ZnO Heterostructure

Huei-Min Huang,[a] Chin-Chia Kuo,[a] Chiao-Yun Chang,[a] Yuan-Ting Lin,[b] Tien-Chang Lu,[a,z] Li-Wei Tu,[b] and Wen-Feng Hsieh[a]

[a] *Department of Photonics, National Chiao Tung University, Hsinchu 30050, Taiwan*
[b] *Department of Physics, National Sun Yat-Sen University, Kaohsiung 80424, Taiwan*

We report on growth and characteristics of *a*-plane GaN/ZnO/GaN epitaxial structures, which can be applied to various optoelectronic devices. The unique optical transitions intrinsic to heterovalent interfaces were found and analyzed. Clear carrier localization effect in the GaN/ZnO heterointerface is observed from the S-shaped energy shift with increasing temperature in the temperature-dependent photoluminescence measurement. The carrier localization also results in strong luminescent intensity and dominates the emission spectrum at room temperature. In addition, the acceptor level originated from the Zn out-diffusion from the ZnO layer is observed in the low temperature photoluminescence spectra, and its binding energy is estimated to be about 0.311 eV.
© 2012 The Electrochemical Society. [DOI: 10.1149/2.080203jes] All rights reserved.

Manuscript submitted October 14, 2011; revised manuscript received December 14, 2011. Published January 10, 2012; publisher error corrected November 14, 2012.

The wide bandgap ZnO has attracted extensive attention due to their superior characteristics in optoelectronics[1] and piezoelectronics.[2] Moreover, many physical properties are very similar to GaN, such as almost the same lattice constant and thermal expansion coefficient, and a quite large room temperature bandgap of 3.30 eV to be close to GaN. Based on their similar properties, the related ZnO/GaN-based heterojunctions have been investigated to realize high performance optoelectronic devices.[3–5] Although investigations of ZnO/GaN heterojunctions are quite readily available, GaN epilayers are still difficult to be deposited on the ZnO layer. It is due to the chemical vulnerability of ZnO at high temperature required for the growth. The weak thermal stability of ZnO, out-diffusion of the Zn atom from ZnO into the GaN epilayer, and H_2 etching phenomenon will cause the poor quality and the rough surface for the GaN epilayer during the conventional chemical vapor deposition growth.[6,7] Therefore, the H_2 free growth and the relatively low temperature growth have been proposed to improve the crystal quality of GaN on ZnO by molecular beam epitaxy (MBE)[8] or pulsed laser deposition (PLD).[9] Moreover, fabrication of the typical GaN/ZnO heterostructure commonly utilizes the ZnO bulk substrate as the template for investigations. However, growth of GaN on the epitaxial ZnO layer using sapphire substrates may provide a cost-effective method to fabricate versatile high performance GaN/ZnO based optoelectronic devices.

It is attractive to use the non-polar growth orientation to avoid polarization in the GaN or ZnO quantum wells or interfaces.[10] Since the lattice mismatches between the wurtzite structure GaN and ZnO are 1.9% along the *c*-axis direction and 0.4% along the *a*-axis direction, it has the potential for the coherent growth of GaN epilayer on ZnO layer even if the growth direction is along the non-polar orientation direction such as *a*-plane (11–20) and *m*-plane (1–100). So far, the non-polar orientation GaN/ZnO heterostructure have been reported,[11,12] and these investigations are mainly focused on developing the effective deposition method and optimizing the crystal quality. However, the related interface characteristics and the optical properties are still not yet clear. In addition, almost all non-polar GaN/ZnO heterostructures were fabricated on the high quality ZnO bulk substrate. Few studies focus on the epitaxial non-polar GaN/ZnO heterostructures on the sapphire substrate at present. The objective of this work is to demonstrate the non-polar *a*-plane GaN layer deposited on the ZnO epitaxial layer by using the plasma-assisted molecular beam epitaxy (PAMBE) system to form the epitaxial growth of GaN/ZnO heterostructure and to clarify the energy levels and the various optical transitions in the *a*-plane GaN/ZnO heterostructure. The interactions between GaN and ZnO layer during growth are also discussed further.

[z] E-mail: timtclu@mail.nctu.edu.tw

To fabricate the non-polar *a*-plane GaN/ZnO heterostructure, firstly, a 2.0-μm-thick *a*-plane GaN layer was grown on *r*-plane sapphire by metal organic chemical vapor deposition (MOCVD). Afterwards, a ZnO film of thickness about 400–500 nm was grown on the *a*-plane GaN template by pulsed laser deposition. The growth temperature was set at 520°C, and the commercial hot-pressed stoichiometric ZnO (99.99% purity) target was focused by a KrF excimer laser ($\lambda = 248$ nm) with the laser energy density of 5–7 J/cm^2. Finally, the GaN epilayer was grown on ZnO/GaN structure in a PAMBE system. Under the H_2 free atmosphere, the GaN epilayer was grown at the temperature of 600°C which is higher than ZnO growth temperature, using a single-step growth without any buffer layer.

After the growth, the X-ray diffraction (XRD) θ-2θ angular scans were utilized to determine the crystalline orientation and to clarify the structures. Figure 1 shows the XRD θ-2θ profile for the structures of ZnO/GaN (ZG) and of GaN/ZnO/GaN (GZG), respectively. The sapphire (1–102), (2–204), GaN (11–20), and ZnO (11–20) reflections are clearly detected from the ZG structure, as shown in Fig. 1a. No GaN (0002) reflection corresponding to $2\theta = 34.604°$ is observed, which indicates that the coherent growth of the ZG structure has been successfully prepared for the following GaN epilayer growth. Subsequently, the GaN epilayer was grown on the ZG structure, and its XRD θ-2θ scan had also been carried out and is shown in Fig. 1b. Besides the original reflections appeared in Fig. 1a, some additional reflections are obviously detected from the GZG structure, as shown in Fig. 1b. Compared with the measurement results of these two structures, the ZnO (11–20) reflection seems to be weaker. Moreover, $ZnGa_2O_4$ (220) and Ga_2O_3 related reflections are observed and identified. It indicates that the ionized Zn and O diffused from the ZnO underlayer may be incorporated into the top GaN epilayer, forming intermediate phases at the GaN/ZnO interface.

Figure 2 is the cross-section scanning electron microscopy (SEM) image of the GZG structure. According to the SEM image, GaN epilayer was indeed deposited on the ZG structure and some micro-air-voids can be observed in the ZnO layer. However, the thickness of ZnO epilayer is greatly reduced from the original 400–500 nm to about 150 nm. It could be believed that the diminution of the thickness is associated with the thermal decomposition of the ZnO epilayer. Simultaneously, the ZnO (11–20) reflection is seen only as a shoulder on the GaN (11–20) reflection profile, as shown in Fig. 1b. Compared with the XRD data and SEM image, the ZnO layer indeed suffers from some damages such as the ZnO bonding decomposition and the ionized element diffusion effect during the GaN layer growth.

Figure 3a shows the PL spectra measured on the GZG and ZG structures at room temperature. Two obvious emission peaks measured from the spectra of the GZG structure lie at about 3.42 eV (P_1) and

Downloaded on 2014-04-28 to IP 140.113.38.11 address. Redistribution subject to ECS terms of use (see ecsdl.org/site/terms_use) unless CC License in place (see abstract).

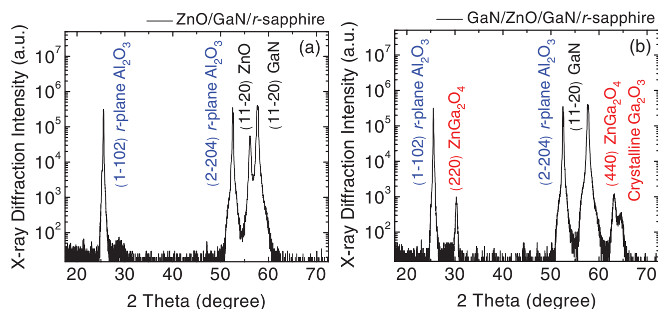

Figure 1. XRD θ-2θ scans of *a*-plane (a) ZnO/GaN/*r*-sapphire and (b) GaN/ZnO/GaN/*r*-sapphire structures.

3.22 eV (P_2), respectively. It is so different from the PL spectrum dominated by the 3.28 eV (P_3) emission peak in the ZG structure. The P_3 emission in the ZG structure is originated from the ZnO layer. Based on these spectra, the P_1 emission is clearly attributed to the optical transition of the GaN layer. On the other hand, the related optical transitions of the P_2 emission peak have been further clarified by performing the temperature-dependent PL measurement ranging from 10 to 295 K, as shown in Fig. 3b. In the low temperature, the emission peak at 3.476 eV corresponds to *a*-plane GaN near band-edge (NBE) emission consisted of two emission peaks assigned to donor-bound exciton (D^0X) and free-exciton (FX) recombination, respectively.[13] If we suppose the free exciton energy of GaN to be 3.476 eV at low temperature, the corresponding bandgap energy will be located at around 3.502 eV with an exciton binding energy of ∼26 meV. This value is very close to the reported GaN fundamental bandgap energy of 3.503 eV at low-temperature by using the temperature dependence optical measurements.[14]

The P_2 emission peak shifts to 3.265 eV as the temperature is lowered to 10 K. Moreover, as the increasing temperature provides the thermal energy for ionized excitons dissociation, the P_2 emission peak still dominates the PL spectrum even at the room temperature. The emission peak is attributed to the carrier localization (E_{local}) at the GaN/ZnO interface with a type II band configuration, which could be due to the formation of interface states and the excess charges from heterovalent bonding.[15,16] The S-shaped P_2 emission peak position variation as a function of the temperature is a typical indication of the carrier localization behavior,[17] as shown in Fig. 3c. Based on these, the P_2 should be assigned to the radiative recombination of carriers localized at the interface. In addition, the low temperature emission peaks at about 3.192 eV and 3.106 eV decrease rapidly with increasing temperature, which are assigned to the band-to-acceptor (*e*A) transition and a donor-acceptor-pairs-like (DAP-like) transition, respectively. The zinc element diffusion phenomenon has been exhibited in the XRD θ-2θ scan, and Zn impurity in GaN (Zn_{Ga}) could behave as the acceptor levels, or as p-type dopant in GaN. It is known that basal stacking faults (BSFs), the quite common defects in *a*-plane GaN-based materials, could be regard as the donors in this case, as a result of the high concentration of donors in the vicinity of BSFs.[18] BSFs-related emission have also been demonstrated to locate at around 3.417–3.420 eV.[13,19] Moreover, the binding energy of Zn_{Ga} in GaN has been determined to be about 0.34 ± 0.04 eV by simulation and experimental measurement,[20,21] which is close to our experimental value of 0.311 eV (= 3.503 eV−3.192 eV). The DAP-like emission energy at around 3.106 eV is almost consistent with the value obtained from the difference between the emission position of BSFs-induced donor-like levels and binding energy of Zn_{Ga} acceptors (3.417 eV−0.311 eV = 3.106 eV).

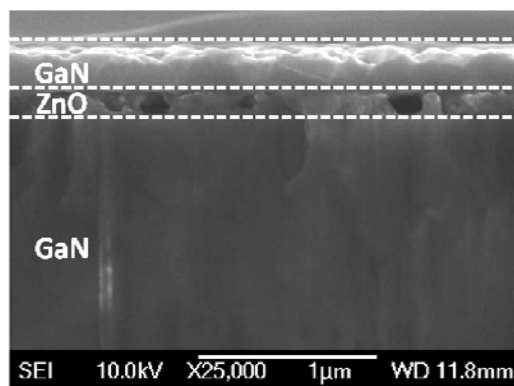

Figure 2. Cross-section SEM image of *a*-plane epitaxial GaN/ZnO/GaN structure.

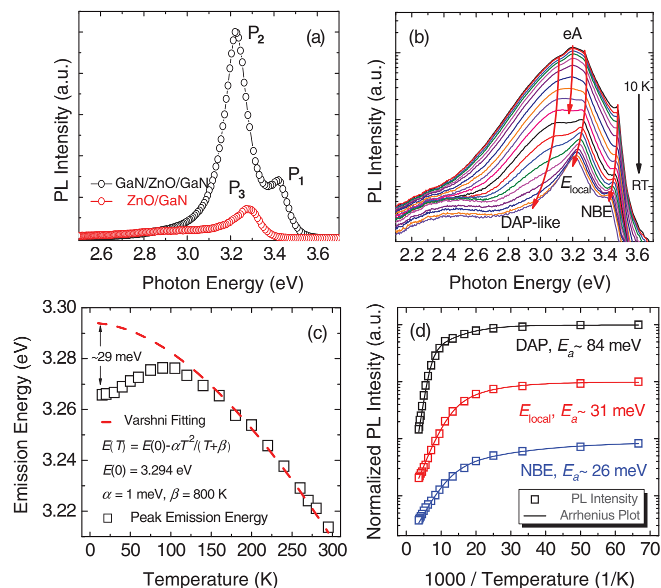

Figure 3. (a) Room-temperature (295 K) PL spectrum of the *a*-plane GaN/ZnO/GaN structure. (b) Temperature-dependent PL spectra ranging from 10 K to 295 K measured from GaN/ZnO/GaN structure. (c) The PL peak energy of the carrier localization as a function of the temperature shows a well Varshni's fitting for the experimental data. (d) The Arrhenius plots of the integrated PL intensities for the *a*-plane GaN/ZnO/GaN structure.

Further the Arrhenius plots of the integrated PL intensities as a function of inverse temperature are summarized in Fig. 3d. The thermal activation energies can be determined by the equation,

$$I = I_0/(1 + A\exp(-E_{a1}/kT) + B\exp(-E_{a2}/kT)),$$

where E_{a1} and E_{a2} are the thermal activation energies at low and high temperature regions, respectively. I_0 is the PL intensity at low temperature, and the coefficients A and B are the rate constants. The thermal activation energy of NBE emission is about 26 meV. This fitted value is assigned to the exciton binding energy of GaN and can correspond to our experimentally measured activation energy. For the transition of the carrier localization, the estimated value of thermal activation energy is about 31 meV, which is close to the localization energy of 29 meV by Varshni's empirical formula, as shown in Fig. 3c, and thus this value could be associated with the carrier delocalization energy with increasing temperature. The BSFs-induced donor level is located about 86 meV below the principle conduction band edge at 10 K, which is close to the fitted value of thermal activation energy of DAP-like transition (about 84 meV). Thus, we can reasonably attribute that thermal activation energy for quenching of DAP-like transition could be the thermal ionization energy of the BSFs-induced donor. Based on the optical measurement results at low temperature, the related energy levels and corresponding optical transitions in *a*-plane GZG structure are sketched in Fig. 4.

Downloaded on 2014-04-28 to IP 140.113.38.11 address. Redistribution subject to ECS terms of use (see ecsdl.org/site/terms_use) unless CC License in place (see abstract).

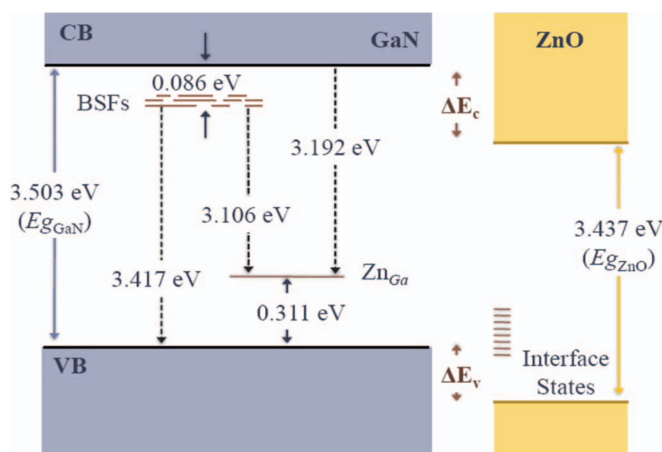

Figure 4. Energy diagram showing the energy levels of Zn-induced acceptors in the *a*-plane GaN on ZnO heterointerface.

In summary, *a*-plane GaN/ZnO/GaN heterostructure has been fabricated by the expitaxial growth techniques, and their optical properties have also been clarified and summarized. The strong emission peak position at around 3.22 eV at room temperature corresponds to the carrier localization at the GaN/ZnO interface. The out-diffusion behavior of Zn atom greatly affects the optical properties of GaN/ZnO, and the binding energy of Zn_{Ga} acceptors is estimated to be about 0.311 eV in the *a*-plane heterostructure. The GaN/ZnO heterostructure is expected to exhibit a significant effect on the recombination at the interface and energy level alignment, and consequently the optoelectronic device application.

Acknowledgments

The author thank Professor. H. C. Kuo and Professor S. C. Wang in Department of Photonics of National Chiao Tung University for their great technical support. This work was supported by the MOE ATU program and in part by the National Science Council of Republic of China (ROC) in Taiwan under contract NSC-99-2120-M-009-007 and NSC 99-2221-E-009-035-MY3.

References

1. P. Yang, H. Yan, S. Mao, R. Russo, J. Johnson, R. Saykally, N. Morris, J. Pham, R. He, and H. J. Choi, *Adv. Funct. Mater.*, **12**(5), 323 (2002).
2. Z. L. Wang and J. Song, *Science*, **312**, 242 (2006).
3. Ya. I. Alivov, J. E. Van Nostrand, D. C. Look, M. V. Chukichev, and B. M. Ataev, *Appl. Phys. Lett.*, **83**, 2943 (2003).
4. Q. X. Yu, B. Xu, Q. H. Wu, Y. Liao, G. Z. Wang, R. C. Fang, H. Y. Lee, and C. T. Lee, *Appl. Phys. Lett.*, **83**, 4713 (2003).
5. D. K. Hwang, S. H. Kang, J. H. Lim, E. J. Yang, J. Y. Oh, J. H. Yang, and S. J. Park, *Appl. Phys. Lett.*, **86**, 222101 (2005).
6. N. Li, E. H. Park, Y. Huang, S. Wang, A. Valencia, B. Nemeth, J. Nause, and I. Ferguson, *Proc. of SPIE*, **6337**, 63370Z (2006).
7. S. J. Wang, N. Li, E. H. Park, Z. C. Feng, A. Valencia, J. Nause, M. Kane, C. Summers, and I. Ferguson, *Phys. stat. sol. (c)*, **5**(6), 1736 (2008).
8. X. Gu, M. A. Reshchikov, A. Teke, D. Johnstone, H. Morkoc, B. Nemeth, and J. Nause, *Appl. Phys. Lett.*, **84**, 2268 (2004).
9. A. Kobayashi, Y. Kawaguchi, J. Ohta, H. Fujioka, K. Fujiwara, and A. Ishii, *Appl. Phys. Lett.*, **88**, 181907 (2006).
10. P. Waltereit, O. Brandt, A. Trampert, H. T. Grahn, J. Menniger, M. Ramsteiner, M. Reiche, and K. H. Ploog, *Nature*, **406**, 865 (2000).
11. A. Kobayashi, S. Kawano, Y. Kawaguchi, J. Ohta, and H. Fujioka, *Appl. Phys. Lett.*, **90**, 041908 (2007).
12. A. Kobayashi, S. Kawano, K. Ueno, J. Ohta, H. Fujioka, H. Amanai, S. Nagao, and H. Horie, *Appl. Phys. Lett.*, **91**, 191905 (2007).
13. P. P. Paskov, R. Schifano, B. Monemar, T. Paskova, S. Figge, and D. Hommel, *J. Appl. Phys.*, **98**, 093519 (2005).
14. B. Monemar, *Phys. Rev. B*, **10**, 676 (1974).
15. T. Nakayama and M. Murayama, *J. Cryst. Growth*, **214/215**, 299 (2000).
16. A. M. C. Ng, Y. Y. Xi, Y. F. Hsu, A. B. Djuri˘si´c, W. K. Chan, S. Gwo, H. L. Tam, K. W. Cheah, P. W. K. Fong, H. F. Lui, and C. Surya, *Nanotechnology*, **20**, 445201 (2009).
17. Y. H. Cho, G. H. Gainer, A. J. Fischer, J. J. Song, S. Keller, U. K. Mishra, and S. P. DenBaars, *Appl. Phys. Lett.*, **73**, 1370 (1998).
18. P. Corfdir, P. Lefebvre, J. Ristić, J. D. Ganière, and B. Deveaud-Plédran, *Phys. Rev. B*, **80**, 153309 (2009).
19. P. Corfdir, P. Lefebvre, J. Levrat, A. Dussaigne, J. D. Ganie`re, D. Martin, J. Ristic´, T. Zhu, N. Grandjean, and B. D. Ple´dran, *J. Appl. Phys.*, **105**, 043102 (2009).
20. M. Monemar, H. P. Gislason, and O. Lagerstedt, *J. Appl. Phys.*, **51**, 640 (1980).
21. N. Nepal, M. L. Nakarmi, H. U. Jang, J. Y. Lin, and H. X. Jiang, *Appl. Phys. Lett.*, **89**, 192111 (2006).

Downloaded on 2014-04-28 to IP 140.113.38.11 address. Redistribution subject to ECS terms of use (see ecsdl.org/site/terms_use) unless CC License in place (see abstract).